Evaluating meso-scale particle movement in gyratory compaction tests of railroad ballasts

Yuanjie Xiao[1, 2*], M. Wang[1], Z. Chang[1], K. Zheng[1], L. Chen[1], and X. Chen[1,2]

[1] School of Civil Engineering, Central South University, Changsha, China
[2] Ministry of Education Key Laboratory for Heavy Haul Railway Engineering Structures, Changsha, China
[*] Corresponding author: yjxiao@csu.edu.cn

ABSTRACT

The quality of compaction of large-sized ballast particles with uniform gradation plays a vital role in trackbed performance of heavy-haul railroads; however, there are currently no unanimously-accepted techniques or quality control criteria available for ensuring adequate compaction of railroad ballasts in either laboratory experiments or field practices. This paper presented preliminary results of a laboratory gyratory compaction study where a real-time particle motion sensor (i.e., SmartRock) was employed to investigate particle movement characteristics during ballast compaction process and provide preliminary meso-scale explanation about compaction mechanisms. The typical ballast gradation commonly used in heavy-haul railroads in China was adopted with different packing structures introduced for comparison. Ballast specimens with varying gradations were prepared and subjected to gyratory compaction. The SmartRock sensors were embedded in representative locations of the specimens to provide meso-scale ballast particle movement and kinematics in terms of rotation, translation (through double integration of acceleration), and orientation in 9 degrees of freedom, whereas the morphological changes of ballast particles after gyratory compaction were quantified using a three-dimensional laser scanner. The results of this study can provide technical insights and guidance to field compaction of ballast layers in heavy-haul railroads.

Keywords: laboratory gyratory compaction;SmartRock sensors; meso-scale

1 INTRODUCTION

The quality of compaction of large-sized ballast particles with uniform gradation contributes to density, uniformity, volumetric property, particle packing structure/arrangement, formation of load-transferring skeleton, and mechanical behavior of ballast layers. The compaction of unbound aggregates including railroad ballasts has been commonly performed with impact, vibratory, gyratory techniques. The gyratory compaction test was originally developed for hot mix asphalt mixtures (Harman et al. 2002) but has also been found effective for unbound granular materials. Gyratory compaction on soils was performed and found to provide more comprehensive information of the compacted materials than impact compaction (Coyle and West 1956; McRae 1965; Zhang et al. 2017). Recently, Li et al. (2015) demonstrated that the gyratory compactor with PDA facilitates characterizing unique moisture-density-energy-strength relationships for waste materials. However, this gyratory compaction approach has not been widely used in compacting soils due to lack of standardization of the gyration variables (such as number of gyrations, gyration angle, rate of gyrations, etc.).

This study is motivated to explore the potential of gyratory compaction for use in ballast aggregates due to the selection of the compaction stress and the output of a complete record of specimen height and shear resistance change with number of gyrations for the compacted specimens. In order to better understand the mechanisms of different compaction methods, this study utilized a recently developed SmartRocks sensoring technology to track meso-scale particle movement and correlate it with compaction variables.

2 LABORATORY GYRATORY COMPACTION TESTS OF BALLAST MATERIALS

2.1 Materials tested

The original ballast gradation has the maximum particle size of more than 60 mm and thus cannot work with the commercial gyratory compactor that is commonly used for hot mix asphalt. Therefore, it was scaled using the procedure described by Wang et al. (2018). The scaled ballast gradation, as well as other three different gradations representing typical ballast packing structures (i.e., floating dense, skeleton dense, and skeleton gap), are shown in Figure 1.

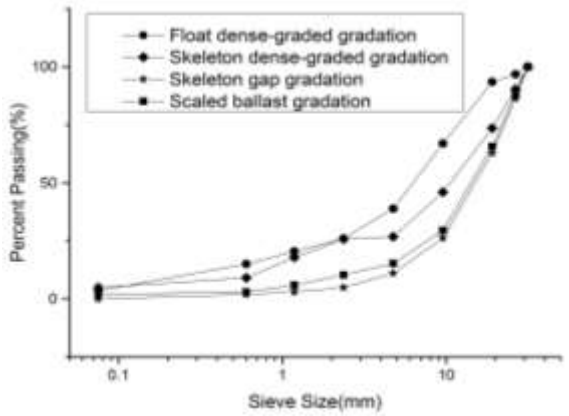

Figure 1. Gradation curves of different ballast packing structures studied

2.3 Gyratory compaction curves of ballast materials

The ballast materials were also compacted in the laboratory by using the gyratory compactor that is designed for compacting hot mix asphalt. It is clearly shown in Figure 2(a) that the specimens with the scaled ballast gradation experienced the greatest magnitude and rate of height decrease during the given 200 gyration cycles.As far as the achieved dry density values shown in Figure 2(b) are concerned, the effectiveness of the gyratory compaction for the four different gradations studied follows the descending order of skeleton dense, floating dense, skeleton gap, and the scaled ballast gradation, respectively.

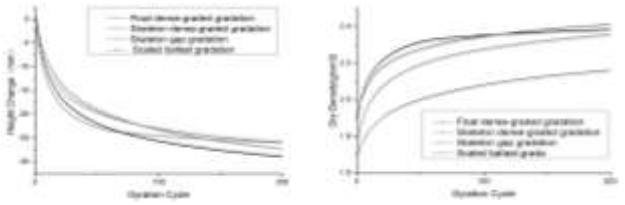

(a) (b)

Figure 2. The gyratory compaction curves of tested ballast materials: (a) Change in specimen height versus the number of gyration cycles and (b) achieved dry density versus the number of gyration cycles

In order to study the effect of gyratory compaction pressure on the compaction quality, the specimens with the scaled ballast gradation were prepared and subjected to different levels of gyratory compaction pressure (i.e., 700, 800, 900, and 1000 kPa). It is clear that increasing gyratory pressure levels results in greater degree of compaction as defined as the ratio of the achieved dry density to the maximum dry density. Further increase in gyratory pressure beyond 800 kPa tends to show relatively insignificant increase in the achieved dry density for specimens with scaled ballast gradation at optimum water content. On the other hand, the rate of specimen height change corresponding to the scaled ballast gradation at the optimum water content of 2.0% is insensitive to the gyratory compaction pressure as shown in Figure 3(b). There also seems to exist two compaction stages as indicated by the rate of specimen height change (see Figure 3b): the initial stage where the abruptly decreasing rate is observed and the second stage where the rate reaches stabilization after a certain number of gyration cycles. Therefore, it becomes reasonable to fix the gyratory pressure at 800 kPa in subsequent compaction tests.

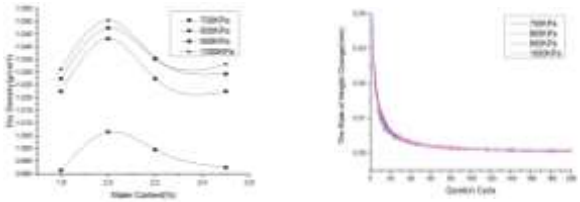

(a) (b)

Figure 3. The gyratory compaction curves of specimens with scaled ballast gradation at optimum water content: (a) effect of varying compaction pressure levels and (b) the rate of specimen height change versus the number of gyration cycles

2.4 Quantification of ballast particle morphology and its variation

In order to quantify the effects of ballast particle morphology and its variation on gyratory compaction quality, a laser scanner was employed to digitize ballast particles retained on No. 4 (or 4.75 mm) sieve and build their three-dimensional (3D) models. This step was performed before and after gyratory compaction so that the changes in ballast particle morphology during gyratory compaction can also be quantified by comparing the differences between the reconstructed digital ballast particles.

2.5 Real-time monitoring of ballast particle movement at meso-scale

The application of such SmartRock sensors in ballasted track has been documented by Huang et al. (2018). Multiple SmartRock sensors were placed at predetermined locations of gyratory specimens to monitor meso-scale ballast particle movement and kinematics in terms of rotation, translation (through double integra-tion of acceleration), and orientation in 9 degrees of freedom.

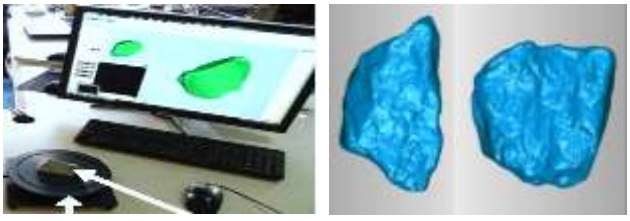

(a) (b)

laser scanner, and (b) photos of reconstructed digital ballast particles

Figure 4. Quantification of ballast particle morphology: (a) 3D

3 RESULTS AND ANAYSIS

3.1 Characteristics of ballast particle movement at meso-scale during gyratory compaction

The particle movement results from the SmartRock sensor placed at the centroid of the gyratory specimen with scaled ballast gradation are plotted in Figure 8. Those data recorded including time histories of Euler angles in all x-, y-, and z-directions, of which a segment of the data output is demonstrated in Figure 5(a)-(c). The time histories of the Euler angles in x- and y-directions exhibit clear cyclic pattern with a period of 2 seconds that matches the rotation frequency of 0.5 Hz and rotation speed of 30 rpm of the gyratory compactor, while there is no cyclic pattern observed for the time history of the Euler angle in z-direction. The relative rotation in each of the three directions, defined as the difference between the maximum and minimum values of the Euler angle for each cycle, is plotted against gyration cycles in Figure 5(d). The evolution trend of the relative rotation during the gyration process is observed to correlate well with those of dry density and specimen height reduction. Obviously, lower and stabilized particle relative rotation indicates stronger particle interlocking and thus less capability of further compaction. From Figure 8(d), it can be seen that particle relative rotation exhibits sharp reduction during the initial stage and then gradually becomes stabilized during the subsequent stage. This is expected because no further compaction effectiveness can be obtained once the particle interlocking is formed and stabilized by initial compaction.

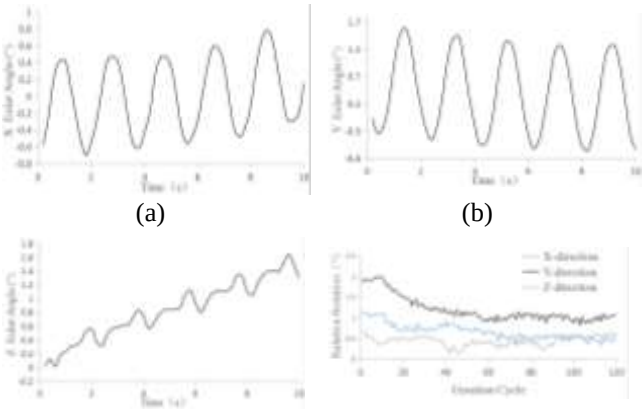

(a) (b)

(c) (d)

Figure 5. Meso-scale ballast particle movement and kinematics recorded by the SmartRock sensor at mid-depth center: (a) x-Euler angle and (b) y- Euler angle, (c) z- Euler angle, and (d) relative rotations in x-, y- and z-directions.

3.2 Effect of ballast particle morphology and its variation on gyratory compaction quality

Those selected sample particles(retained on No. 4 or 4.75 mm sieve) were all digitalized for 3D shape by the aforementioned laser scanner before and after gyratory compaction, respectively. Therefore, it becomes possible to compare 3D shapes of each sample particle and further quantify morphological variation due to the gyratory compaction process.Figure 6 provides representative laser scanning results of this purpose. Figure 6(a) demonstrate one example particles with shape variations (or abrasion depth) due to gyratory compaction coded by different colors. It can be clearly seen that the most significant abrasion occurs near the sharp corners. As shown in Figure 6(b), particles that are of greater size or subjected to higher compaction pressure levels are more prone to abrasion or breakage.

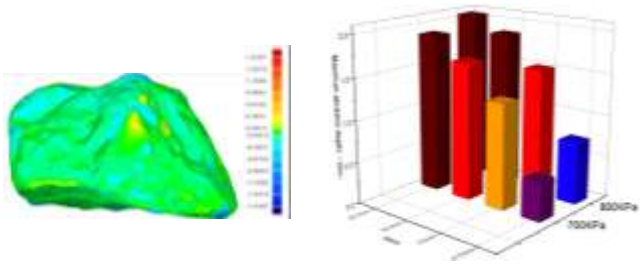

(a) (b)

Figure 6. Illustration of quantification of particle morphological variation for gyratory specimens with scaled ballast gradation and optimum moisture content of 2%: (a) one sample particle,and (b) maximum particle abrasion depth of different sizes versus compaction pressure level.

3.3 Gradation variation during gyratory compaction process

The gyratory specimens were all subjected to mechanical sieve analysis to determine the gradation curves before and after gyratory compaction and thus evaluate particle breakage and gradation variation. It can be seen from Figure 7 that the gradation variations for the floating dense and skeleton dense gradations are relatively much less than those for the skeleton gap and scaled ballast gradations, which can also be observed from specimens after gyratory compaction.

The degree of particle breakage can be defined by Hardin (1985) is widely accepted as a technique that adequately integrates particle breakage index (PBI) over a wide size fraction. The PBI is quantified by the parameter B_r that is formulated by Equation 1, where B_{pi} and B_{pf} are defined as the areas formed by the following three lines: the grain size distribution curve before or after gyratory compaction tests, a horizontal line passing 100% finer, and a vertical line passing the No. 200 sieve (0.075 mm), respectively.

$$B_r = \frac{B_{pi} - B_{pf}}{B_{pi}} \qquad (1)$$

where B_r = relative breakage index (PBI); B_p = breakage potential; B_{pi} = pre-test breakage potential; B_{pf} = post-test breakage potential.

It is evident that the highest particle breakage potential at both compaction pressure levels is found for the skeleton gap gradation, followed sequentially by

scaled ballast, skeleton dense, and floating dense gradation types as shown figure 8.

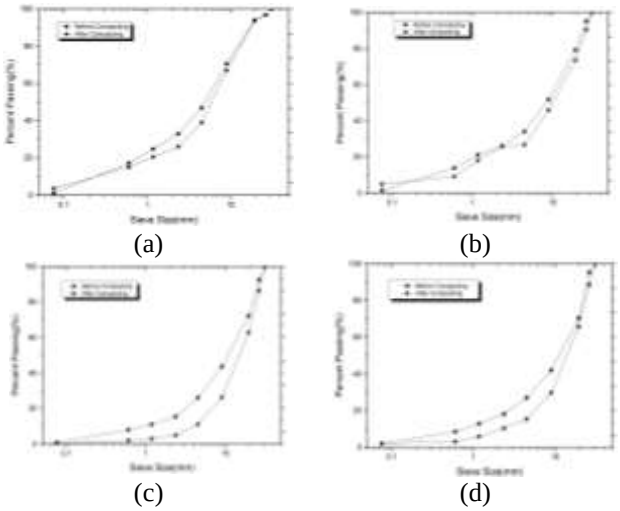

(a) (b) (c) (d)

Figure 7. Gradation curves of gyratory specimens measured before and after gyratory compaction: (a) floating dense, (b) skeleton dense, (c) skeleton gap, and (d) scaled ballast gradation.

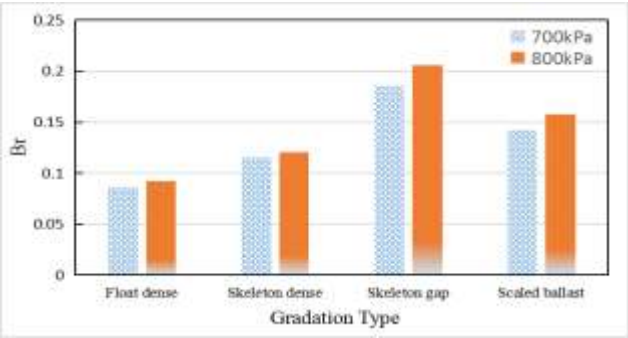

Figure 8. Particle Breakage Index (B_r) values calculated for different gradation types at two compaction pressure levels during gyratory compaction.

4 SUMMARY AND CONCUSIONS

This work investigated the approach of using a gyratory compactor along with the SmartRocks sensor and 3D laser scanner as a means to linking the compaction variables with particle morphology and meso-scale particle movement for compacted ballast aggregate materials. Based on the results of tests and analysis, the following conclusions can be drawn:

- Particle rotation and translation behaviors were measured, correlated with compaction variables, and then used to well explain compaction mechanisms of different gradation types.
- The relative rotation pattern of the particles along x- and y-directions was directly related to material density change and specimen height change during gyratory compaction.
- From the relative rotation curves along x- and y-directions, the compaction process can be divided into initial compaction stage, transition stage, and stabilization (or plateau) stage.
- The quantified particle morphology and gradation variations, as well as particle breakage potential, were also found to well correlate with compaction variables and thus contribute to the meso-scale explanation of compaction mechanisms.

Future work might also explore the possibility of using the real time SmartRock sensor technique to monitor the density change for field compaction, study the correlation between laboratory and field compaction, and seek possibilities to improve both laboratory and field compaction.

ACKNOWLEDGMENTS

The work presented in this paper is financially supported by the National Natural Science Foundation of China (Grant No. 51878673). The authors are also grateful to Prof. Hai Huang (Penn State Altoona) and STARDAL Company for providing SmartRocks products and necessary technical support.

References

Coyle, H. M., and West, E. C. (1956). “Laboratory compaction of a silty clay to simulate field density curves.” M.S. thesis, Massachusetts Institute of Technology, Cambridge, MA.

Y. L.Guo,Valeri Markine,J.N.Song, G.Q.Jing(2018)Ballast degr adation: Effect of particle size and shape using los Angeles Abrasion test and image analysis.Construction of Building Materials ,169,414-424

Hardin, B. O. (1985). “Crushing of soil particles.” J. Geotech. Engrg., 10.1061/(ASCE)0733-9410(1985)111:10(1177), pp. 1177–1192.

Leslie, D.D. (1975). "Shear Strength of Rockfill," Physical Properties Engineering Study No. 526, South Pacific Division, Corps of Engineers Laboratory, Sausalito, CA.

Li, C., White, D. J., and Vennapusa, P. (2015). “Moisture-density-strength-energy relationships for gyratory compacted geomaterials.” Geotech. Test. J., 38(4), 461–473.

McRae, J. L. (1965). “Gyratory testing machine technical manual for bituminous mixtures, soils, and base course materials.” Engineering Developments Company, Inc., Vicksburg, MA.

H. -L. Wang, Y.-J. Cui, F. Lamas-Lopez, N. Calon, G. Saussine, J.-C. Dupla, J. Canou, P. Aimedieu, R.-P. Chen (2018). “Investigation on the mechanical behavior of track-bed materials at various contents of coarse grains.” Construction and Building Materials 164 (2018) 228–237

H.L.Wang.,Y.J.Cui.,R.P.Chen.(2018). “Investigation on the mechanical behavior of track-bed materials at various contents of coarse grains.” Construction of Building Materials, 164, 228-237

X. Wang, S.H. Shen, H. Huang, and Luiz C.A. (2018). “Characterization of particle movement in superpave gyratory compactor at meso-scale using SmartRock sensors.” Construction of Building Materials, 164, 206-214

C. Zhang, H.N., Wang, Z.P. You, X. Yang (2016). “Compaction characteristics of asphalt mixture with different gradation type through Superpave Gyratory Compaction and X-Ray CT Scanning.” Construction of Building Materials, 129, 243-255

Zhang, J., White, D.J., and Vennapusa, P.K.R. (2017). “Estimating Mechanistic Parameters for Subgrade Using Gyratory Compaction with Pressure Distribution Analyzer.” J. Mater. Civ. Eng., 2017, 29(11): 04017216